



Anger recall mental stress decreases ^{123}I -metaiodobenzylguanidine (^{123}I -MIBG) uptake and increases heterogeneity of cardiac sympathetic activity in the myocardium in patients with ischemic cardiomyopathy

Ricardo Avendaño, MD,^a Taraneh Hashemi-Zonouz, MD,^a Veronica Sandoval, BS,^b Chi Liu, PhD,^{c,d} Matthew Burg, PhD,^a Albert J. Sinusas, MD,^{a,b,c,d} Rachel Lampert, MD,^a and Yi-Hwa Liu, PhD^{a,b,e}

^a Section of Cardiovascular Medicine, Department of Internal Medicine, Yale University School of Medicine, New Haven, CT

^b Nuclear Cardiology Laboratory, Yale-New Haven Hospital, New Haven, CT

^c Department of Radiology and Biomedical Imaging, Yale University School of Medicine, New Haven, CT

^d Department of Biomedical Engineering, Yale University School of Medicine, New Haven, CT

^e Department of Biomedical Engineering, Chung Yuan Christian University, Taoyuan, Taiwan

Received Jan 8, 2020; Revised Aug 28, 2020; accepted Aug 31, 2020

doi:10.1007/s12350-020-02372-1

Background. Acute psychological stressors such as anger can precipitate ventricular arrhythmias, but the mechanism is incompletely understood. Quantification of regional myocardial sympathetic activity with ^{123}I -metaiodobenzylguanidine (^{123}I -mIBG) SPECT imaging in conjunction with perfusion imaging during mental stress may identify a mismatch between perfusion and sympathetic activity that may exacerbate a mismatch between perfusion and sympathetic activity that could create a milieu of increased vulnerability to ventricular arrhythmia.

Methods. Five men with ischemic cardiomyopathy (ICM), and five age-matched healthy male controls underwent serial ^{123}I -mIBG and $^{99\text{m}}\text{Tc}$ -Tetrofosmin SPECT/CT imaging during an anger recall mental stress task and dual isotope imaging was repeated approximately 1 week later during rest. Images were reconstructed using an iterative reconstruction algorithm with CT-based attenuation correction. The mismatch of left ventricular myocardial ^{123}I -mIBG and $^{99\text{m}}\text{Tc}$ -Tetrofosmin was assessed along with radiotracer heterogeneity and the ^{123}I -mIBG heart-to-mediastinal ratios (HMR) were calculated using custom software developed at Yale.

Electronic supplementary material The online version of this article (<https://doi.org/10.1007/s12350-020-02372-1>) contains supplementary material, which is available to authorized users.

Ricardo Avendaño and Taraneh Hashemi-Zonouz have contributed equally to this work.

The authors of this article have provided a PowerPoint file, available for download at SpringerLink, which summarizes the contents of the paper and is free for re-use at meetings and presentations. Search for the article DOI on SpringerLink.com.

The authors have also provided an audio summary of the article, which is available to download as ESM, or to listen to via the JNC/ASNC Podcast.

Funding: This work was supported in part by two Investigator Initiated Trial Grants from General Electric Healthcare, Inc. (M150714,

Lampert13-MIBG-004Grants, Lampert & Liu), two Grant-in-Aid research grants from the American Heart Association (13GRNT17090037 Chi Liu and 14GRNT19040010, Y-H Liu), NIH R01 Grant (R01 HL084438, Burg), and NIH T32 training Grant (HL098069, Sinusas). No other potential conflict of interest relevant to this article was reported.

Reprint requests: Yi-Hwa Liu, PhD, Section of Cardiovascular Medicine, Department of Internal Medicine, Yale University School of Medicine, Dana 3, PO Box 208017, New Haven, CT 06520-8017; yi-hwa.liu@yale.edu

1071-3581/\$34.00

Copyright © 2020 American Society of Nuclear Cardiology.

Results. The hemodynamic response to mental stress was similar in both groups. The resting-HMR was greater in healthy control subjects (3.67 ± 0.95) than those with ICM (3.18 ± 0.68 , $P = .04$). Anger recall significantly decreased the HMR in ICM patients (2.62 ± 0.3 , $P = .04$), but not in normal subjects. The heterogeneity of ¹²³I-mIBG uptake in the myocardium was significantly increased in ICM patients during mental stress ($26\% \pm 8.23\%$ vs. rest: $19.62\% \pm 9.56\%$; $P = .01$), whereas the ^{99m}Tc-Tetrofosmin uptake pattern was unchanged.

Conclusion. Mental stress decreased the ¹²³I-mIBG HMR, increased mismatch between sympathetic activity and myocardial perfusion, and increased the heterogeneity of ¹²³I-mIBG uptake in ICM patients, while there was no significant change in myocardial defect size or the heterogeneity of ^{99m}Tc-Tetrofosmin perfusion. The changes observed in this proof-of-concept study may provide valuable information about the trigger–substrate interaction and the potential vulnerability for ventricular arrhythmias. (J Nucl Cardiol 2022;29:798–809.)

Key Words: ¹²³I-mIBG • HMR • Sympathetic activation • Ventricular arrhythmia • Sudden cardiac death

Abbreviations

HMR	Heart-to-mediastinal ratio
ICD	Implantable cardioverter defibrillator
ICM	Ischemic cardiomyopathy
¹²³ I-mIBG	¹²³ I-metaiodobenzylguanidine
LV	Left ventricle
LVEF	Left ventricular ejection fraction
SCD	Sudden cardiac death
SPECT	Single-photon emission computed tomography
^{99m} Tc	Technetium-Tc99m
VA	Ventricular arrhythmia

INTRODUCTION

Sudden cardiac death (SCD) is a significant contributor to overall mortality in the general population.¹ While the majority of SCD events occur in individuals with no known history of cardiovascular disease,² underlying coronary artery disease (CAD) plays a vital role in the incidence of SCD.^{2–6} The relationship between psychological stress and SCD is well established and is increased during emotionally impactful events such as natural disasters, major sporting events, or terrorists attacks.^{7–11} Similarly, mental stress incited by anger can also trigger ventricular arrhythmias.¹² We have previously reported in a laboratory study that performance of mentally stressful tasks increases sympathetic activation,^{13–15} and those with the most significant increases in sympathetically mediated electrophysiological changes were most likely to have life-threatening ventricular arrhythmias.¹⁶ However, the pathophysiological links between stress-induced sympathetic activation and SCD have not been fully defined and require further investigation.

¹²³I-metaiodobenzylguanidine (¹²³I-mIBG) is an established radiotracer for detection of the sympathetic

innervation in the heart^{17–19} that can be imaged using planar or single-photon emission computed tomography (SPECT) for assessment of the risk of ventricular arrhythmias (VA) and SCD in patients with ICM^{20–25} and for prediction of mortality in patients with heart failure (HF).^{26–28} While the majority of ¹²³I-mIBG imaging has been restricted to the assessment of global indices of sympathetic function and its association with VA,^{29,30} there appears to be a high correlation between innervation/perfusion mismatch and incidence of VA in patients with ICM.³¹ Lautamaki et al demonstrated the relationship between innervation/perfusion mismatch and vulnerability of VA using multi-isotope PET imaging.³² Other investigators, using SPECT imaging in combination with electrophysiological (EP) testing reported that decreased uptake of ¹²³I-mIBG in the infarct border zone was associated with VA inducibility.³³ Based on these prior studies demonstrating associations of abnormal ¹²³I-MIBG indices and both clinical and induced arrhythmia, we hypothesized that anger provocation could increase sympathetic-perfusion mismatch as measured by ¹²³I-mIBG SPECT imaging in conjunction with ^{99m}Tc-tetrofosmin SPECT imaging in patients with ICM at risk for SCD who had previously received an implantable cardioverter defibrillator (ICD). Based on the known mechanistic role of electrical heterogeneity in arrhythmogenesis,^{16,34–37} we also investigated a new ¹²³I-MIBG marker of heterogeneity of sympathetic activation in exploratory fashion.

METHODS

Following the approval of the Yale Human Investigations Committee, we prospectively enrolled ten patients (all males, ages 59.7 ± 7.6 years) at the Yale New Haven Hospital. All subjects signed a written informed consent form. Five patients from an ongoing study of mental stress in patients with cardiomyopathy

and implanted defibrillators underwent the addition of MIBG imaging after modification of that protocol. (R01HL084438) As the funding for this pilot study was limited, a homogeneous group was chosen which included male patients with ischemic myopathy over 55 years old. Controls were healthy age- and sex-matched volunteers, drawn from a study developing a normal database for MIBG.³⁸ Hemodynamic variables were measured continuously throughout the imaging protocol for both the rest and mental stress studies in all subjects. Blood samples for catecholamine analysis were drawn at the rest and stress and analyzed at the Yale Center for Clinical Investigation.

Mental Stress Protocol

As shown in Figure 1, all subjects underwent sequential ^{123}I -mIBG and $^{99\text{m}}\text{Tc}$ -tetrofosmin ECG-gated SPECT imaging during mental stress, and follow-up dual isotope SPECT imaging at rest on a separate day approximately 1 week later. All subjects underwent our standard anger recall mental stress protocol³⁹ in two separate occasions within the same day at the time of ^{123}I -mIBG and $^{99\text{m}}\text{Tc}$ -tetrofosmin injection and imaging as shown in Figure 1. This stress protocol has been shown to be highly reproducible if performed in two separate occasions.⁴⁰ During the stress day, the room lights were dimmed to maintain a quiet environment. In the baseline period, starting at least 30 minute after the intravenous (IV) placement, patients were encouraged to think about past relaxing situations, followed by a 10-minute period of anger recall. For the latter, patients described a recent event eliciting irritation, annoyance, or frank anger, with the insertion of frequent irritating questions by the interviewer to facilitate a re-experiencing of the event. For stress imaging, the radiotracers were injected at 5 minute into the period of provoked anger recall. One week later, sequential rest ^{123}I -mIBG and $^{99\text{m}}\text{Tc}$ -tetrofosmin SPECT images were acquired with an identical acquisition imaging protocol, starting 30 minute after IV insertion, with patients instructed to think of relaxing situations throughout. The left ventricular ejection fraction (LVEF) was measured from the 3D ECG-gated $^{99\text{m}}\text{Tc}$ -tetrofosmin SPECT images at each time experimental timepoint using Yale SPECT quantification software.⁴¹

SPECT ^{123}I -mIBG Imaging and Analysis

All subjects underwent five 15-minute dynamic SPECT scans at 0, 30, 90, 120, and 180 minute after injection of ^{123}I -mIBG 235.32 ± 66.6 MBq (6.36 ± 1.8 mCi). The images acquired at the critical early time point were used for data analysis, since this

reflects the time of maximal hemodynamic response to mental stress, increases in circulating catecholamines, and precedes the generation of radiotracer metabolites. SPECT data were acquired in raw listmode with a 32×32 matrix and 2.5×2.5 mm² pixel size for 15 minute with 10% energy window ($\pm 5\%$) centered at the ^{123}I photopeak (159 keV) using a stationary cardiac-dedicated hybrid SPECT/CT scanner equipped with cadmium zinc telluride (CZT) detectors and 19 tungsten pinhole collimators (Discovery NM/CT 570c; GE Healthcare). A non-contrast CT scan was acquired for nonuniform attenuation correction of SPECT images using the following acquisition parameters: 120 kVp, 60 mA, pitch of 0.984, slice thickness of 2.5 mm, and rotation speed of 0.4 s. X-ray CT images were reconstructed using filtered backprojection with a voxel size of 0.977 mm³ and SPECT images were reconstructed with a matrix size of 70×70 and pixel size of 3.2×3.2 mm² using the maximum-likelihood expectation maximization algorithm with the CT-based attenuation correction.

For SPECT/CT ^{123}I -mIBG imaging quantification, the upper and lower limits of the heart were determined by the central transaxial slice of CT images co-registered with SPECT, and the volume of interest (VOI) of the left ventricle (LV) was automatically segmented using a previously published bimodal median threshold algorithm.^{42,43} Mean counts in the LV myocardium were calculated from the LV regions segmented, and mean counts of the background were calculated from the mediastinal volume with a fixed size of $5 \times 5 \times 5$ voxels manually defined. This approach, has yielded results that correlate and are highly reproducible with the more conventional planar imaging methods.³⁸ The approach for quantification of the HMR from SPECT images is illustrated in Figure 2.

SPECT/CT ^{123}I -mIBG defect sizes derived from all slices were summed to calculate the total myocardial perfusion defect size (%LV) for the entire LV and inhomogeneity of tracer uptake was used as an exploratory measure of heterogeneity of cardiac sympathetic innervation. Inhomogeneity was defined as a percent variability (standard deviation divided by mean counts) derived from the three regional circumferential count profiles (base, mid-ventricular and apical) of the short-axis SPECT slices generated by the Yale quantification software.⁴¹

SPECT $^{99\text{m}}\text{Tc}$ -Tetrofosmin Imaging and Analysis

SPECT data were acquired in raw listmode for 15 min at 30 min post $^{99\text{m}}\text{Tc}$ -Tetrofosmin 351.5 ± 21.46 MBq (9.5 ± 0.58 mCi) injection with

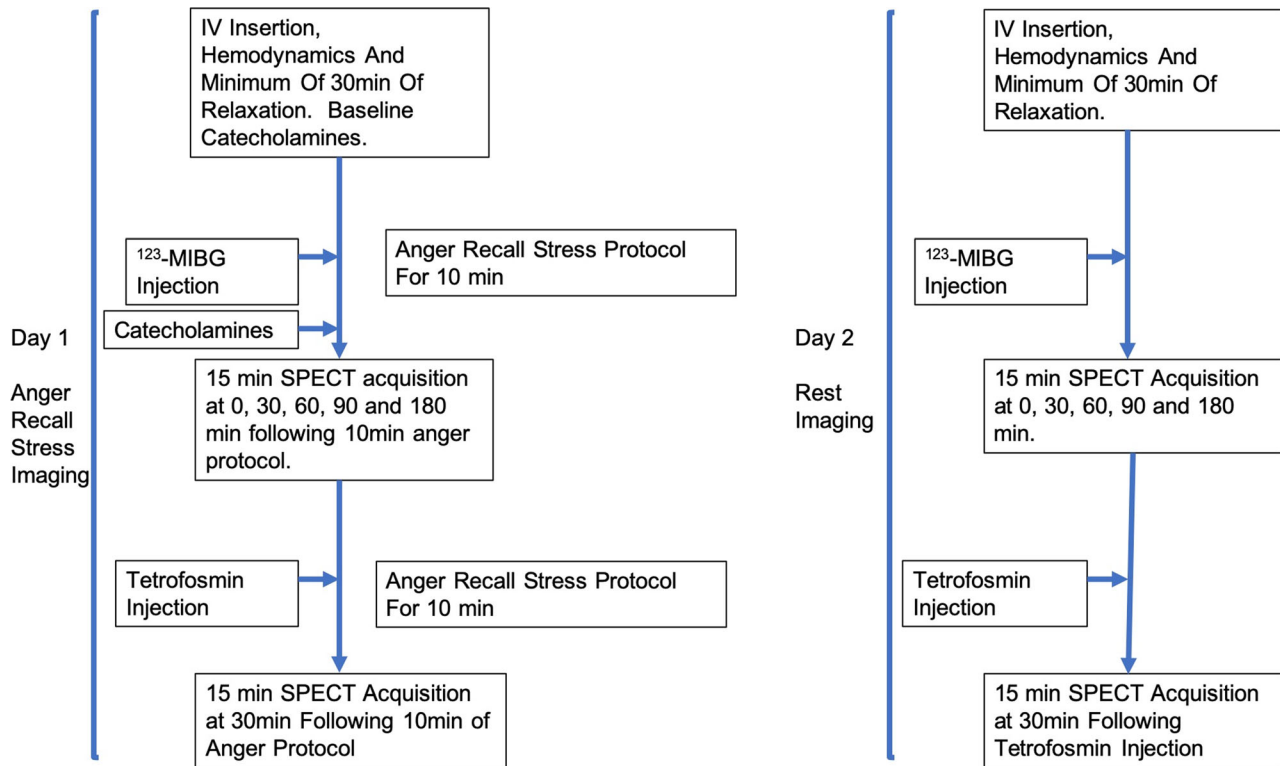


Figure 1. Schematic diagram of the study protocol.

10% energy window ($\pm 5\%$) centered at the ^{99m}Tc photopeak (140 keV) using the same hybrid SPECT/CT scanner and imaging protocol as those used in the ¹²³I-MIBG imaging. Images were reconstructed with the same parameters as used in the ¹²³I-MIBG SPECT/CT reconstructions described above. Myocardial perfusion defect size and LVEF were determined from the reconstructed SPECT images using the Yale SPECT quantification software,⁴¹ based on the circumferential count profiles of SPECT images.⁴⁴ In brief, circumferential count profiles were generated slice-by-slice from the radial sectors of SPECT short-axis slices via maximal count sampling. Each circumferential count profile was normalized to the peak value of the corresponding count profile. Lower limit of normal (LLN) radiotracer distribution was calculated as the mean minus 2 standard deviations (SD) of the normalized count profiles, derived from the Yale Nuclear Cardiology Laboratory database of healthy normal volunteers. The normalized circumferential count profiles from patients were compared against the profiles of the LLN distribution on a slice-by-slice basis to calculate myocardial perfusion defect size via integrating the area between the normalized circumferential count profiles of patients and the LLN profiles. Ultimately, the defect sizes derived from all slices were summed to calculate

the total myocardial perfusion defect size (%LV) for the entire LV.

Statistical Analysis

All statistical analyses were performed using GraphPad Prism Version 8. Data were expressed as mean \pm SD in bar graphs. Paired two-tailed *t* test was used to analyze same group analysis and unpaired two-tailed *t* test was used for comparisons of difference between two measures. *P* < .05 was considered as statistically significant in the comparisons.

RESULTS

Population Characteristics and Hemodynamic Response to Mental Stress

The demographic and clinical characteristics of the age-matched healthy controls (*n* = 5, mean age 59.4 ± 5.7) and ICM patients (*n* = 5, mean age 67.0 ± 9.6) are summarized in Table 1. As shown in Table 2, baseline hemodynamics were similar between the two groups. There were no significant differences between ICM patients and controls in hemodynamic

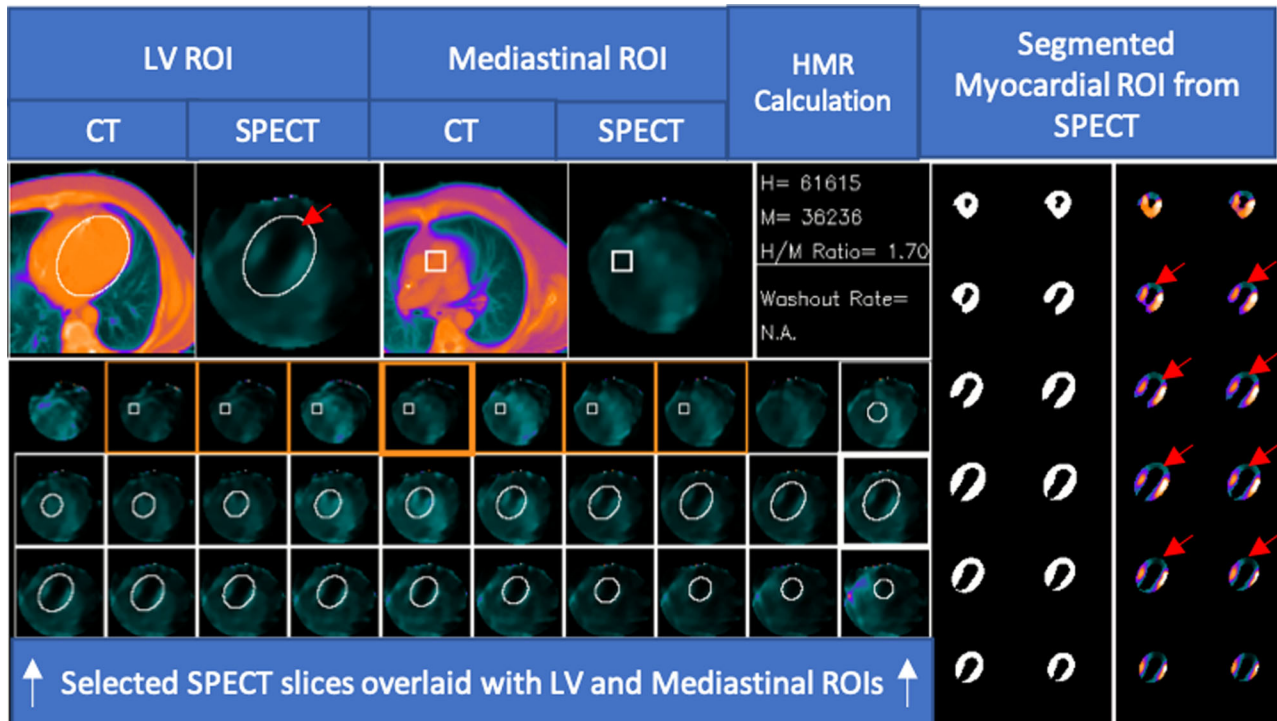


Figure 2. Illustration of our SPECT approach for segmentation and quantification of the HMR for a patient from the ICM group from the hybrid SPECT/CT images. An elliptical region was used to locate heart, and a square ROI was used for determination of mediastinal activity. The binary image represents the mask used for quantification of myocardial uptake. The red arrows indicate the areas of myocardial perfusion defects. Heart-to-mediastinal ratio (HMR), left ventricle (LV), region of interest (ROI).

Table 1. Demographics and clinical characteristics

	Healthy controls (n = 5)	ICM patients (n = 5)
Age (years)	59.4 ± 5.70	67.0 ± 9.61
Male	5 (100%)	5 (100%)
EF%	56.6 ± 1.14	30.8 ± 9.3
CAD	0 (0%)	5 (100%)
HTN	1 (20%)	5 (100%)
DM	0 (0%)	2(40%)
Smoking	1 (20%)	4 (80%)
Medications		
Beta-Blockers	0 (0%)	5(100%)
ACE or ARB	0 (0%)	4 (80%)
CCB	1 (20%)	2 (40%)
Digoxin	0 (0%)	2 (40%)
Amiodarone	0 (0%)	1 (20%)

CAD Coronary Artery Disease, CCB Calcium Channel Blockers, DM Diabetes Mellitus, EF Ejection Fraction, ICM Ischemic Cardiomyopathy, SD Standard Deviation

Table 2. Autonomic and hemodynamic changes with mental stress

	Healthy controls		Ischemic cardiomyopathy patients (ICM)		Change between groups		
	Baseline (B)	Mental stress (MS)	Baseline (B)	Mental stress (MS)	Healthy controls (MS-B)	ICM patients ^b Δ (MS-B)	P
Systolic BP (mmHg)	104.80 ± 3.96	132.60 ± 7.60	107.80 ± 16.07	131 ± 16.11	27.8 ± 6.01	23.2 ± 13.66	.5103
Diastolic BP (mmHg)	63.80 ± 7.15	79.20 ± 7.56	58.40 ± 9.18	68 ± 13.75	15.4 ± 10.24	9.6 ± 7.76	.3424
Heart rate (bpm)	61.40 ± 1.14	68.20 ± 4.91	67.80 ± 7.85	76.40 ± 10.74	6.8 ± 4.76	8.6 ± 7.63	.6666
Norepinephrine (pg/mL)	294.20 ± 121.70	412.20 ± 129.60	357.20 ± 81.16	515.80 ± 141.10	118 ± 74.97	158.6 ± 183.3	.6589

response to anger recall mental stress for between-group comparisons. Within-group analysis showed significant changes with the stress in systolic and diastolic blood pressure, heart rate and norepinephrine levels in controls, while in the ICM group, only the change in systolic blood pressure reached the statistical significance.

¹²³I-MIBG HMR AT BASELINE AND DURING ANGER RECALL

Baseline ¹²³I-mIBG HMR was lower in the ICM patients (3.18 ± 0.68) versus control subjects (3.67 ± 0.95, *P* = .37) as shown in Figure 3. Anger recall mental stress significantly decreased HMR (from 3.18 ± 0.68 to 2.62 ± 0.63, *P* = .04) in ICM patients but not in the controls (from 3.67 ± 0.96 to 3.48 ± 0.59, *P* = .76), with a significant between-group difference in change in HMR with stress, *P* = .04).

¹²³I-MIBG UPTAKE RELATIVE TO PERFUSION AT BASELINE AND DURING ANGER RECALL

Representative rest and anger recall mental stress SPECT ¹²³I-mIBG and ^{99m}Tc-Tetrofosmin images from an ICM patient are shown in Figure 4. Anger recall mental stress was associated with an increase in the ¹²³I-mIBG defect as seen clearly on the horizontal long-axis images, although there was no significant change in ^{99m}Tc-Tetrofosmin perfusion. The average changes in SPECT ¹²³I-mIBG and ^{99m}Tc-Tetrofosmin defect sizes at rest and during stress are shown in Figure 5 for all ICM patients. There was a significant increase in ¹²³I-mIBG defect size for the ICM patients (Figure 5A)

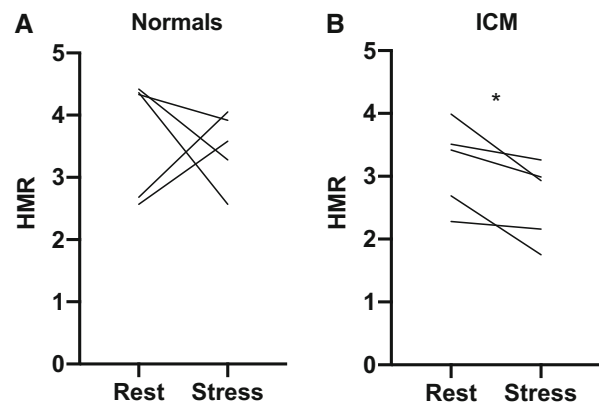


Figure 3. SPECT HMR after mental stress and at rest in normal controls (A) and ICM patients (B). There was a significant decrease in HMR following mental stress compared to baseline in patients with ICM (stress: 2.62 ± 0.63; rest: 3.18 ± 0.68, *P* = .04), between-group difference was significant, *P* = .04.

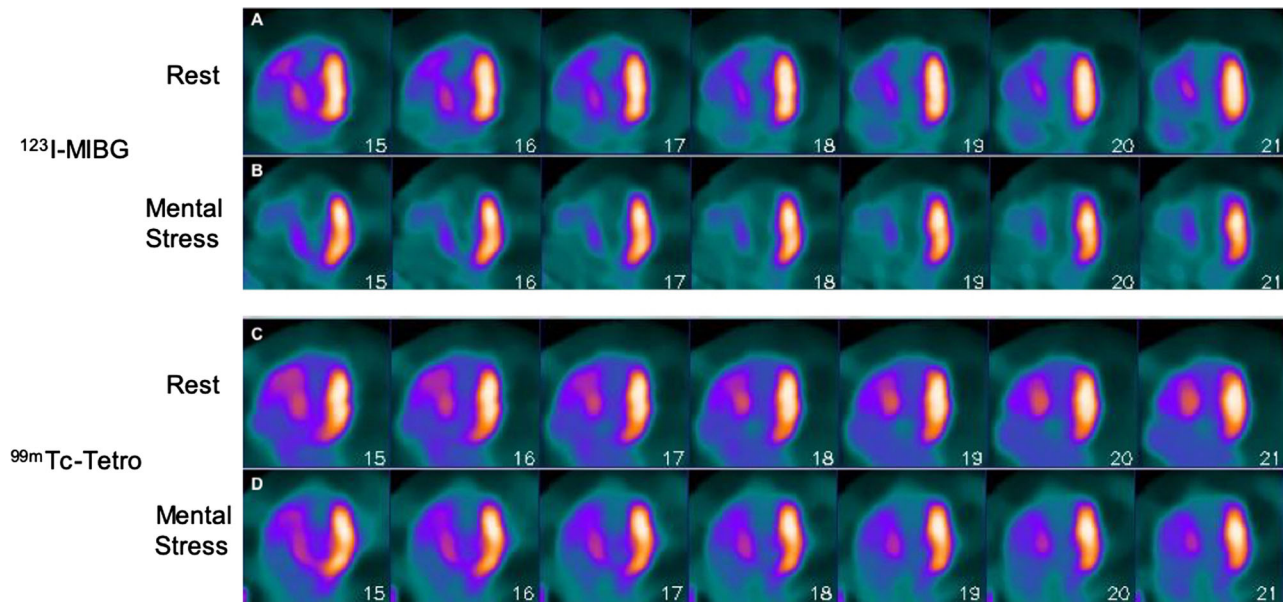


Figure 4. Horizontal long-axis slices of the SPECT acquisition from a patient of the ICM group at rest and mental stress with ^{123}I -mIBG (top) and $^{99\text{m}}\text{Tc}$ -Tetrofosmin (bottom). The transition from the inferior surface of the heart progressing to the anterior surface is displayed from left to right. Following mental stress, there is an increase in ^{123}I -mIBG defect size as evident by a relative decrease in ^{123}I -mIBG uptake to $^{99\text{m}}\text{Tc}$ -Tetrofosmin following anger recall mental stress. There appears to be a change in LV chamber size between rest and stress images.

during anger recall mental stress (rest: $16.2\% \pm 8.29\%$; anger recall mental stress: $25\% \pm 10.1\%$; $P = .02$), whereas the $^{99\text{m}}\text{Tc}$ -Tetrofosmin defect size (Figure 5B) did not change significantly (rest: $14.2\% \pm 7.33\%$; anger recall mental stress: $16.2\% \pm 7.53\%$; $P = .15$). $^{99\text{m}}\text{Tc}$ -Tetrofosmin TID index (transient ischemic dilation) did not demonstrate significant change in LV volume with stress (mean = 1.038; SD = 0.056). The control (normal) patients demonstrated no perfusion defects at stress or rest.

Heterogeneity of Myocardial ^{123}I -mIBG Uptake

The heterogeneity of myocardial ^{123}I -mIBG uptake calculated for the apical, mid-ventricular, and basal regions of the myocardium during the rest and mental stress in both normal and ICM patients is summarized in Figure 6. The percentage variability of ^{123}I -mIBG uptake in the apical and mid-ventricular regions was significantly increased after anger recall mental stress in ICM patients but did not change in the normal control subjects. There were no significant changes observed in the percentage variability of ^{123}I -mIBG uptake in the basal region in either groups. Percentages of uptake per myocardial region are summarized in Table 3.

DISCUSSION

In this study, we found that laboratory-induced recall of a previous incident that provoked anger led to a significant reduction in the HMR of patients with known ICM, whereas the HMR did not change in healthy normal subjects with anger recall stress. In addition, we observed increased heterogeneity of cardiac sympathetic activity in patients with ICM as assessed by quantitative ^{123}I -mIBG SPECT imaging, while the pattern of $^{99\text{m}}\text{Tc}$ -tetrofosmin SPECT perfusion did not significantly change, suggesting that mental stress also induced an increase in sympathetic activity/perfusion mismatch in patients with ICM.

Unlike norepinephrine, ^{123}I -mIBG is an analogue of the false neurotransmitter guanethidine which is not metabolized following intravenous injection and therefore accumulates in the presynaptic terminal,⁴⁵ providing an indirect evaluation of the presynaptic integrity.⁴⁶ The use of ^{123}I -mIBG imaging to evaluate denervated myocardium following myocardial infarction has been extensively reported,^{17–19,21,24}. Furthermore, abnormal ^{123}I -mIBG uptake has been shown to be associated with worse prognosis and death particularly in patients with ICM,^{22,25–28,47} and vulnerability for developing VA.^{29,30,48} Similarly, ^{11}C -hydroxyephedrine (HED) a PET radiotracers has been used to evaluate

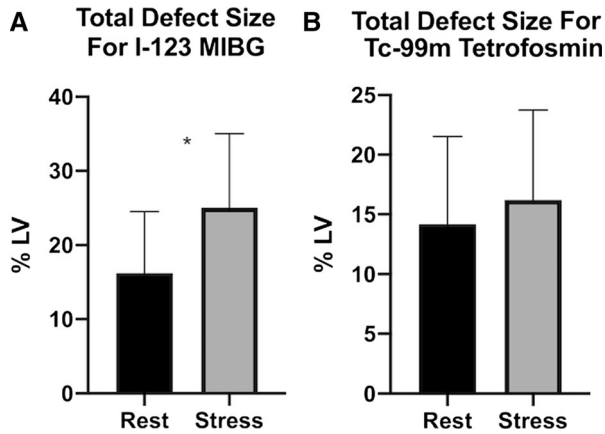


Figure 5. Assessment of SPECT ¹²³I-MIBG (A) and ^{99m}Tc-Tetrofosmin (B) defect sizes at rest and after anger recall mental stress in ICM patients. There was a significant increase in ¹²³I-MIBG defect size in ICM patients after mental stress, although there was no significant change in ^{99m}Tc-Tetrofosmin defect size associated with mental stress.

cardiac sympathetic neuronal function and to predict the specific-mortality from SCD independent of LVEF in patients with ICM.^{49,50} Although the HMR quantified from planar ¹²³I-MIBG images provides a useful global index of cardiac sympathetic innervation,⁵¹ more recently the assessment of the innervation/perfusion mismatch from dual isotope cardiac SPECT may define the potential mechanisms for the association between sympathetic denervation and arrhythmic risk.^{31,52}

While between-group comparisons of hemodynamic response to anger recall showed no difference between ICM patients and healthy controls (Table 2), the significant within-group differences seen in healthy controls but not in the ICM patients might be due to the fact that the majority of the ICM patients were either on betablockade (100%) or anti-hypertensive medications (80%), as these medications have been shown in prior studies to decrease hemodynamic response to mental stress.⁵³ Whether these patients' beta-blockers similarly blunted the effects of anger on the ¹²³I-MIBG uptake is unknown.

For the analysis of the ¹²³I-MIBG data, we focused on the early SPECT images (before 10 min) at which time the anger recall mental stress induced the greatest hemodynamic response. Analysis of this early time point may also be critical since we previously demonstrated that the ¹²³I-MIBG metabolites usually peak between 10 and 15 min after radiotracer injection.⁵⁴ As expected, we also observed a global reduction in the ¹²³I-MIBG HMR in ICM patients compared to the age-matched normal controls. However, ¹²³I-MIBG SPECT imaging of patients with ICM demonstrated heterogeneity of sympathetic activity under resting conditions, which

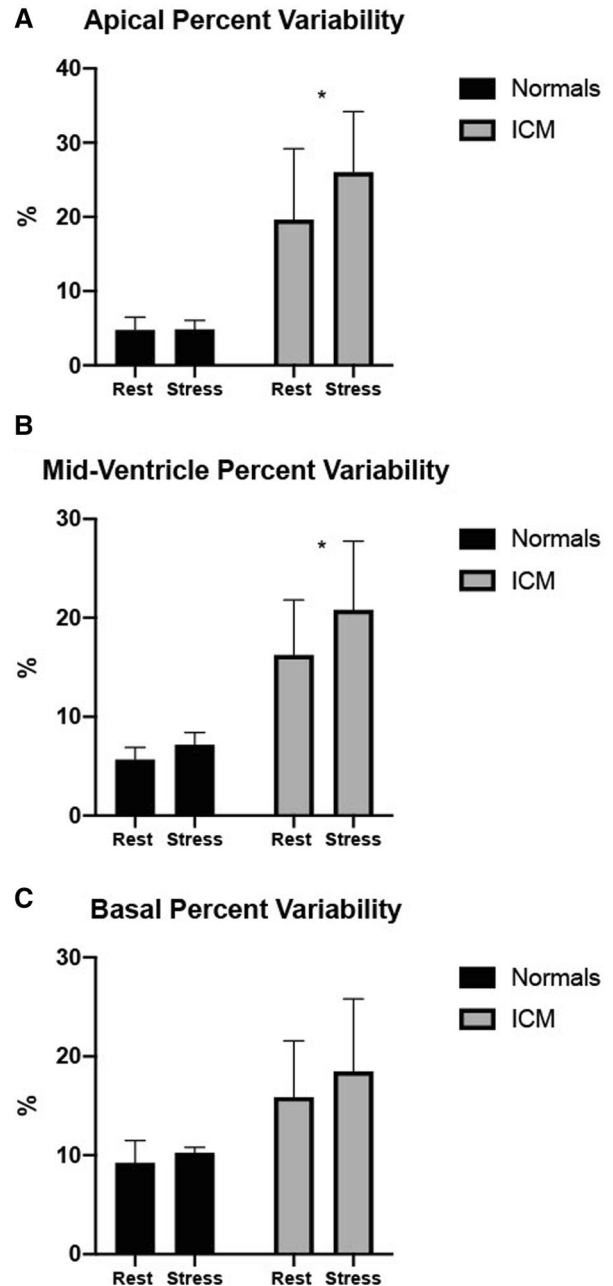


Figure 6. Heterogeneity of myocardial ¹²³I-MIBG uptake in apical (A), mid-ventricular (B), and basal (C) regions during rest and anger recall mental stress in normal controls and ICM patients. The percentage variability of ¹²³I-MIBG uptake in the apical and mid-ventricular regions was significantly increased after mental stress in ICM patients but not in normal control subjects. No significant changes were observed in the percentage variability of ¹²³I-MIBG uptake in the basal region in both groups.

were exacerbated during the anger recall mental stress. More specifically, this change in regional myocardial ¹²³I-MIBG activity with mental stress occurred independent of any changes in regional myocardial

Table 3. Regional heterogeneity of ¹²³I-mIBG uptake

	Healthy controls			Ischemic cardiomyopathy patients (ICM)			Change between groups		
	Baseline (B)	Mental stress (MS)	P	Baseline (B)	Mental stress (MS)	P	Healthy controls Δ (B-MS)	ICM patients Δ (B-MS)	P
Apical region (%)	4.78 ± 1.70	4.83 ± 1.20	.9461	19.62 ± 9.55	26 ± 8.23	.0079	0.05 ± 1.73	6.38 ± 2.89	.0030
Mid-ventricular region (%)	5.69 ± 1.19	7.15 ± 1.25	.1143	16.26 ± 5.53	20.78 ± 6.94	.0127	1.45 ± 1.61	4.51 ± 2.35	.0433
Basal region (%)	9.24 ± 2.24	10.27 ± 0.52	.4435	15.88 ± 5.67	18.48 ± 7.30	.1599	1.02 ± 2.69	2.60 ± 3.37	.4364

perfusion, resulting in regional innervation/perfusion mismatch.

The changes in regional myocardial ¹²³I-mIBG uptake, independent of ^{99m}Tc-tetrofosmin perfusion, increases in heterogeneity of local myocardial sympathetic activity under conditions of psychological stress may guide speculation into pathways through which stress precipitates ventricular arrhythmias, as previously shown.^{7,12} Stress and increases in catecholamines increase electrical heterogeneity¹⁶ which in turn is associated with arrhythmogenesis.^{26,28–30,55} Our findings suggest that stress-induced heterogeneity of local sympathetic activity could potentially underlie the increases in electrical heterogeneity seen with stress. Furthermore, previous experimental studies have also demonstrated that the sympathetic nervous system modulates heterogeneity of cardiac conduction, through promoting lateralization of connexins near the infarct border zone which are thought to augment conduction and thus promotes heterogeneity in electrical activation and propagation.⁵⁶ Further, heterogeneity of ¹²³I-mIBG uptake in the border zone or scar tissue has been shown to be associated with inducibility of VA on electrophysiologic studies.³³

Clinical Implications

While the data are most relevant as a proof-of-concept study in helping to elucidate mechanisms underlying the previously demonstrated increase in electrical heterogeneity with mental stress,^{16,34–37} there are possible clinical implications that should be further studied in larger cohorts to confirm the results. Over the past three decades, several studies have reported the usefulness of ¹²³I-mIBG imaging for the assessment, prognostication and risk stratification many clinical populations, particularly in those with heart failure.^{17–19,21,22,25,27–31}

It is possible that mental rest/stress dual isotope ¹²³I-MIBG and ^{99m}Tc-tetrofosmin SPECT imaging could further improve the predictive value of ¹²³I-MIBG imaging in identifying patients at risk for SCD. Arrhythmias require both substrate and trigger, and assessments which include how triggering factors interact with substrate may provide more predictive value than assessments measuring substrate alone.

LIMITATIONS

The proof-of-concept study has several limitations among which the main limitations are the small sample size and the highly selected population. All studies were done with anger on the first day, and rest 1 week later, in order to minimize contamination of the rest phase with

anticipatory anxiety and novelty. We cannot exclude the possibility that patients were anxious even though the setting was no longer novel; were this the case, the true impact of stress on the MIBG parameters may be stronger than demonstrated.

While age matching among the two cohorts was performed as closely as possible, there remained an 8-year difference and the possibility that age contributed to the differences seen can be excluded. Some,⁵⁷ but not all,^{58–61} prior studies have shown MIBG abnormalities in healthy elderly individuals. In addition, whether or not women would demonstrate similar responses as seen in the present study may require further investigation.

Finally, despite abundant evidence demonstrating the use of ¹²³I-mIBG imaging for the characterization of cardiac sympathetic denervation and prediction of future arrhythmia, the clinical use of ¹²³I-mIBG remains limited in the United States.

NEW KNOWLEDGE GAINED

The present study showed an association between psychological stress and alterations in the ¹²³I-mIBG HMR and an increased mismatch in perfusion and denervation, as well as increase in heterogeneity of ¹²³I-mIBG uptake in patients with ICM. These findings may improve our understanding of the interaction between a stress trigger and underlying substrate in ways which promote arrhythmogenesis.

CONCLUSIONS

In this proof-of-concept study, anger recall mental stress resulted in a significant decline in the ¹²³I-mIBG HMR for ICM patients, and an increase in the heterogeneity of sympathetic activation for these patients, that was not associated with changes in myocardial perfusion, findings which may help elucidate the electrical changes seen previously with stress. Further research is needed to determine whether the use of non-invasive dual isotope ¹²³I-mIBG and ^{99m}Tc-tetrofosmin SPECT/CT imaging during a mental stress protocol can help further stratify patients at risk for the development of VA and SCD.

Acknowledgements

We thank Vera Tsatkin, Ramesh Fazzone-Chettiar, and Stephanie Thorn, PhD, for their technical assistance in this study.

Disclosures

This work was supported in part by two Investigator Initiated Trial Grants from General Electric Healthcare, Inc.

(M150714, Lampert; 13-MIBG-004Grants, Lampert & Liu), two Grant-in-Aid research grants from the American Heart Association (13GRNT17090037, Chi Liu and 14GRNT19040010, Yi-Hwa Liu), NIH R01 Grant (R01HL084438, Burg), and NIH T32 training Grant (HL098069, Sinusas). Ricardo Avendaño does not have any potential conflict of interest relevant to disclose, Taraneh Hashemi-Zonouz does not have any potential conflict of interest relevant to disclose, and Rachel Lampert does not have any potential conflict of interest relevant to disclose.

References

1. Hayashi M, Shimizu W, Albert CM. The spectrum of epidemiology underlying sudden cardiac death. *Circ Res.* 2015;116:1887–906.
2. Chugh SS, Reinier K, Teodorescu C, Evano A, Kehr E, Al Samara M, et al. Epidemiology of sudden cardiac death: Clinical and research implications. *Prog Cardiovasc Dis.* 2008;51:213–28.
3. Hinkle LE Jr, Thaler HT. Clinical classification of cardiac deaths. *Circulation.* 1982;65:457–64.
4. Weisfeldt ML, Everson-Stewart S, Sitlani C, Rea T, Aufderheide TP, Atkins DL, et al. Ventricular tachyarrhythmias after cardiac arrest in public versus at home. *N Engl J Med.* 2011;364:313–21.
5. Chugh SS, Jui J, Gunson K, Stecker EC, John BT, Thompson B, et al. Current burden of sudden cardiac death: multiple source surveillance versus retrospective death certificate-based review in a large U.S. community. *J Am Coll Cardiol.* 2004;44:1268–75.
6. Olson KA, Patel RB, Ahmad FS, Ning H, Bogle BM, Goldberger JJ, et al. Sudden cardiac death risk distribution in the United States population (from NHANES, 2005 to 2012). *Am J Cardiol.* 2019;123:1249–54.
7. Leor J, Poole WK, Kloner RA. Sudden cardiac death triggered by an earthquake. *N Engl J Med.* 1996;334:413–9.
8. Katz E, Metzger JT, Marazzi A, Kappenberger L. Increase of sudden cardiac deaths in Switzerland during the 2002 FIFA World Cup. *Int J Cardiol.* 2006;107:132–3.
9. Kitamura T, Kiyohara K, Iwami T. The great east Japan earthquake and out-of-hospital cardiac arrest. *N Engl J Med.* 2013;369:2165–7.
10. Uchimura M, Kizuki M, Takano T, Morita A, Seino K. Impact of the 2011 Great East Japan Earthquake on community health: Ecological time series on transient increase in indirect mortality and recovery of health and long-term-care system. *J Epidemiol Community Health.* 2014;68:874–82.
11. Meisel SR, Kutz I, Dayan KI, Pauzner H, Chetboun I, Arbel Y, et al. Effect of Iraqi missile war on incidence of acute myocardial infarction and sudden death in Israeli civilians. *Lancet.* 1991;338:660–1.
12. Lampert R, Joska T, Burg MM, Batsford WP, McPherson CA, Jain D. Emotional and physical precipitants of ventricular arrhythmia. *Circulation.* 2002;106:1800–5.
13. Burg MM, Lampert R, Joska T, Batsford W, Jain D. Psychological traits and emotion-triggering of ICD shock-terminated arrhythmias. *Psychosom Med.* 2004;66:898–902.
14. Lampert R. Behavioral influences on cardiac arrhythmias. *Trends Cardiovasc Med.* 2016;26:68–77.
15. Bernardi L, Wdowczyk-Szulc J, Valenti C, Castoldi S, Passino C, Spadacini G, et al. Effects of controlled breathing, mental activity

- and mental stress with or without verbalization on heart rate variability. *J Am Coll Cardiol.* 2000;35:1462–9.
16. Lampert R, Shusterman V, Burg M, McPherson C, Batsford W, Goldberg A, et al. Anger-induced T-wave alternans predicts future ventricular arrhythmias in patients with implantable cardioverter-defibrillators. *J Am Coll Cardiol.* 2009;53:774–8.
 17. Stanton MS, Tuli MM, Radtke NL, Heger JJ, Miles WM, Mock BH, et al. Regional sympathetic denervation after myocardial infarction in humans detected noninvasively using I-123-metaiodobenzylguanidine. *J Am Coll Cardiol.* 1989;14:1519–26.
 18. McGhie AI, Corbett JR, Akers MS, Kulkarni P, Sills MN, Kremers M, et al. Regional cardiac adrenergic function using I-123 metaiodobenzylguanidine tomographic imaging after acute myocardial infarction. *Am J Cardiol.* 1991;67:236–42.
 19. Henderson EB, Kahn JK, Corbett JR, Jansen DE, Pippin JJ, Kulkarni P, et al. Abnormal I-123 metaiodobenzylguanidine myocardial washout and distribution may reflect myocardial adrenergic derangement in patients with congestive cardiomyopathy. *Circulation.* 1988;78:1192–9.
 20. Estorch M, Flotats A, Serra-Grima R, Mari C, Prat T, Martin JC, et al. Influence of exercise rehabilitation on myocardial perfusion and sympathetic heart innervation in ischaemic heart disease. *Eur J Nucl Med.* 2000;27:333–9.
 21. Matsuo S, Takahashi M, Nakamura Y, Kinoshita M. Evaluation of cardiac sympathetic innervation with iodine-123-metaiodobenzylguanidine imaging in silent myocardial ischemia. *J Nucl Med.* 1996;37:712–7.
 22. Matsui T, Tsutamoto T, Maeda K, Kusukawa J, Kinoshita M. Prognostic value of repeated 123I-metaiodobenzylguanidine imaging in patients with dilated cardiomyopathy with congestive heart failure before and after optimized treatments—comparison with neurohumoral factors. *Circ J.* 2002;66:537–43.
 23. Kasama S, Toyama T, Kumakura H, Takayama Y, Ichikawa S, Suzuki T, et al. Spironolactone improves cardiac sympathetic nerve activity and symptoms in patients with congestive heart failure. *J Nucl Med.* 2002;43:1279–85.
 24. Hartikainen J, Mantysaari M, Kuikka J, Lansimies E, Pyorala K. Extent of cardiac autonomic denervation in relation to angina on exercise test in patients with recent acute myocardial infarction. *Am J Cardiol.* 1994;74:760–3.
 25. Wakabayashi T, Nakata T, Hashimoto A, Yuda S, Tsuchihashi K, Travin MI, et al. Assessment of underlying etiology and cardiac sympathetic innervation to identify patients at high risk of cardiac death. *J Nucl Med.* 2001;42:1757–67.
 26. Jacobson AF, Senior R, Cerqueira MD, Wong ND, Thomas GS, Lopez VA, et al. Myocardial iodine-123 meta-iodobenzylguanidine imaging and cardiac events in heart failure. Results of the prospective ADMIRE-HF (AdreView Myocardial Imaging for Risk Evaluation in Heart Failure) study. *J Am Coll Cardiol.* 2010;55:2212–21.
 27. Merlet P, Benvenuti C, Moyses D, Pouillart F, Dubois-Rande JL, Duval AM, et al. Prognostic value of MIBG imaging in idiopathic dilated cardiomyopathy. *J Nucl Med.* 1999;40:917–23.
 28. Momose M, Kobayashi H, Iguchi N, Matsuda N, Sakomura Y, Kasanuki H, et al. Comparison of parameters of 123I-MIBG scintigraphy for predicting prognosis in patients with dilated cardiomyopathy. *Nucl Med Commun.* 1999;20:529–35.
 29. Arora R, Ferrick KJ, Nakata T, Kaplan RC, Rozengarten M, Latif F, et al. I-123 MIBG imaging and heart rate variability analysis to predict the need for an implantable cardioverter defibrillator. *J Nucl Cardiol.* 2003;10:121–31.
 30. Paul M, Schafers M, Kies P, Acil T, Schafers K, Breithardt G, et al. Impact of sympathetic innervation on recurrent life-threatening arrhythmias in the follow-up of patients with idiopathic ventricular fibrillation. *Eur J Nucl Med Mol Imaging.* 2006;33:866–70.
 31. Yukinaka M, Nomura M, Ito S, Nakaya Y. Mismatch between myocardial accumulation of 123I-MIBG and 99mTc-MIBI and late ventricular potentials in patients after myocardial infarction: Association with the development of ventricular arrhythmias. *Am Heart J.* 1998;136:859–67.
 32. Lautamaki R, Schuleri KH, Sasano T, Javadi MS, Youssef A, Merrill J, et al. Integration of infarct size, tissue perfusion, and metabolism by hybrid cardiac positron emission tomography/computed tomography: Evaluation in a porcine model of myocardial infarction. *Circ Cardiovasc Imaging.* 2009;2:299–305.
 33. Zhou Y, Zhou W, Folks RD, Manatunga DN, Jacobson AF, Bax JJ, et al. I-123 mIBG and Tc-99m myocardial SPECT imaging to predict inducibility of ventricular arrhythmia on electrophysiology testing: A retrospective analysis. *J Nucl Cardiol.* 2014;21:913–20.
 34. Pastore JM, Girouard SD, Laurita KR, Akar FG, Rosenbaum DS. Mechanism linking T-wave alternans to the genesis of cardiac fibrillation. *Circulation.* 1999;99:1385–94.
 35. Nearing BD, Verrier RL. Modified moving average analysis of T-wave alternans to predict ventricular fibrillation with high accuracy. *J Appl Physiol.* 1985;2002:541–9.
 36. Shusterman V, Goldberg A, London B. Upsurge in T-wave alternans and nonalternating repolarization instability precedes spontaneous initiation of ventricular tachyarrhythmias in humans. *Circulation.* 2006;113:2880–7.
 37. Gehi AK, Stein RH, Metz LD, Gomes JA. Microvolt T-wave alternans for the risk stratification of ventricular tachyarrhythmic events: A meta-analysis. *J Am Coll Cardiol.* 2005;46:75–82.
 38. Alvi R, Miller EJ, Zonouz TH, Sandoval V, Tariq N, Lampert R, et al. Quantification and determination of normal (123I)-metaiodobenzylguanidine heart-to-mediastinum ratio (HMR) from cardiac SPECT/CT and correlation with planar HMR. *J Nucl Med.* 2018;59:652–8.
 39. Lampert R, Jain D, Burg MM, Batsford WP, McPherson CA. Destabilizing effects of mental stress on ventricular arrhythmias in patients with implantable cardioverter-defibrillators. *Circulation.* 2000;101:158–64.
 40. Jain D, Joska T, Lee FA, Burg M, Lampert R, Zaret BL. Day-to-day reproducibility of mental stress-induced abnormal left ventricular function response in patients with coronary artery disease and its relationship to autonomic activation. *J Nucl Cardiol.* 2001;8:347–55.
 41. Liu Y. Quantification of nuclear cardiac images: The Yale approach. *J Nucl Cardiol.* 2007;14:483–91.
 42. Liu Y-H, Zonouz TH, Sandoval V, Lampert R, Sinusas A. Normal limits of heart-to-mediastinum ratio (Hmr) of I-123 mibg uptake quantified from high-sensitivity (Hs) and high-resolution (Hr) spect/Ct. *J Am Coll Cardiol.* 2016;67:1822.
 43. Liu Y-H, Sinusas AJ. Planar versus SPECT quantification of the heart-to-mediastinum ratio from I-123-MIBG sympathetic cardiac SPECT imaging: Accuracy as assessed by computer simulations. *Eur Heart J Cardiovasc Imaging.* 2015;16:20.
 44. Liu YH, Sinusas AJ, DeMan P, Zaret BL, Wackers FJ. Quantification of SPECT myocardial perfusion images: Methodology and validation of the Yale-CQ method. *J Nucl Cardiol.* 1999;6:190–204.
 45. Raffel DM, Wieland DM. Development of mIBG as a cardiac innervation imaging agent. *JACC Cardiovasc Imaging.* 2010;3:111–6.
 46. Sisson JC, Wieland DM. Radiolabeled meta-iodobenzylguanidine: Pharmacology and clinical studies. *Am J Physiol Imaging.* 1986;1:96–103.

47. Nakata T, Miyamoto K, Doi A, Sasao H, Wakabayashi T, Kobayashi H, et al. Cardiac death prediction and impaired cardiac sympathetic innervation assessed by MIBG in patients with failing and nonfailing hearts. *J Nucl Cardiol.* 1998;5:579–90.
48. Calkins H, Allman K, Bolling S, Kirsch M, Wieland D, Morady F, et al. Correlation between scintigraphic evidence of regional sympathetic neuronal dysfunction and ventricular refractoriness in the human heart. *Circulation.* 1993;88:172–9.
49. Fallavollita JA, Heavey BM, Luisi AJ Jr, Michalek SM, Baldwa S, Mashtare TL Jr, et al. Regional myocardial sympathetic denervation predicts the risk of sudden cardiac arrest in ischemic cardiomyopathy. *J Am Coll Cardiol.* 2014;63:141–9.
50. Luisi AJ Jr, Suzuki G, Dekemp R, Haka MS, Toorongian SA, Canty JM Jr, et al. Regional 11C-hydroxyephedrine retention in hibernating myocardium: Chronic inhomogeneity of sympathetic innervation in the absence of infarction. *J Nucl Med.* 2005;46:1368–74.
51. Travin MI, Feng D, Taub CC. Novel imaging approaches for predicting arrhythmic risk. *Circ Cardiovasc Imaging.* 2015;8:e003019.
52. Gimelli A, Menichetti F, Soldati E, Liga R, Scelza N, Zucchelli G, et al. Predictors of ventricular ablation's success: Viability, innervation, or mismatch? *J Nucl Cardiol.* 2019;20:1–9.
53. Steptoe A, Ronaldson A, Kostich K, Lazzarino AI, Urbanova L, Carvalho LA. The effect of beta-adrenergic blockade on inflammatory and cardiovascular responses to acute mental stress. *Brain Behav Immun.* 2018;70:369–75.
54. Wu J, Lin SF, Gallezot JD, Chan C, Prasad R, Thorn SL, et al. quantitative analysis of dynamic 123I-MIBG SPECT imaging data in healthy humans with a population-based metabolite correction method. *J Nucl Med.* 2016;57:1226–32.
55. Coumel P. Cardiac arrhythmias and the autonomic nervous system. *J Cardiovasc Electrophysiol.* 1993;4:338–55.
56. Ajjola OA, Lux RL, Khaheera A, Kwon O, Aliotta E, Ennis DB, et al. Sympathetic modulation of electrical activation in normal and infarcted myocardium: Implications for arrhythmogenesis. *Am J Physiol Heart Circ Physiol.* 2017;312:H608–21.
57. Tsuchimochi S, Tamaki N, Tadamura E, Kawamoto M, Fujita T, Yonekura Y, et al. Age and gender differences in normal myocardial adrenergic neuronal function evaluated by iodine-123-MIBG imaging. *J Nucl Med.* 1995;36:969–74.
58. Asghar O, Arumugam P, Armstrong I, Ray S, Schmitt M, Malik RA. Iodine-123 metaiodobenzylguanidine scintigraphy for the assessment of cardiac sympathetic innervation and the relationship with cardiac autonomic function in healthy adults using standardized methods. *Nucl Med Commun.* 2017;38:44–50.
59. Gill JS, Hunter GJ, Gane G, Camm AJ. Heterogeneity of the human myocardial sympathetic innervation: in vivo demonstration by iodine 123-labeled meta-iodobenzylguanidine scintigraphy. *Am Heart J.* 1993;126:390–8.
60. Roberts G, Lloyd JJ, Jefferson E, Kane JPM, Durcan R, Lawley S, et al. Uniformity of cardiac (123)I-MIBG uptake on SPECT images in older adults with normal cognition and patients with dementia. *J Nucl Cardiol.* 2019;20:1–13.
61. Somsen GA, Verberne HJ, Fleury E, Righetti A. Normal values and within-subject variability of cardiac I-123 MIBG scintigraphy in healthy individuals: Implications for clinical studies. *J Nucl Cardiol.* 2004;11:126–33.

Publisher's Note Springer Nature remains neutral with regard to jurisdictional claims in published maps and institutional affiliations.